WATER RESEARCH 44 (2010) 320–330

Available at www.sciencedirect.com

ScienceDirect

journal homepage: www.elsevier.com/locate/watres

Complementary methods to investigate the development of clogging within a horizontal sub-surface flow tertiary treatment wetland

P.R. Knowles [a,*], P. Griffin [b], P.A. Davies [a]

[a] Sustainable Environment Research Group, Aston University, Birmingham B4 7ET, UK
[b] Severn Trent Water Ltd, Avon House, St.Martins Road, Coventry CV3 6PR, UK

ARTICLE INFO

Article history:
Received 25 July 2009
Received in revised form
7 September 2009
Accepted 10 September 2009
Published online 12 September 2009

Keywords:
Treatment wetlands
Horizontal sub-surface flow
Hydraulic conductivity
Clogging
Tracer tests
Hydrodynamics

ABSTRACT

A combination of experimental methods was applied at a clogged, horizontal subsurface flow (HSSF) municipal wastewater tertiary treatment wetland (TW) in the UK, to quantify the extent of surface and subsurface clogging which had resulted in undesirable surface flow. The three dimensional hydraulic conductivity profile was determined, using a purpose made device which recreates the constant head permeameter test *in-situ*. The hydrodynamic pathways were investigated by performing dye tracing tests with Rhodamine WT and a novel multi-channel, data-logging, flow through Fluorimeter which allows synchronous measurements to be taken from a matrix of sampling points. Hydraulic conductivity varied in all planes, with the lowest measurement of 0.1 m d^{-1} corresponding to the surface layer at the inlet, and the maximum measurement of 1550 m d^{-1} located at a 0.4 m depth at the outlet. According to dye tracing results, the region where the overland flow ceased received five times the average flow, which then vertically short-circuited below the rhizosphere. The tracer break-through curve obtained from the outlet showed that this preferential flow-path accounted for approximately 80% of the flow overall and arrived 8 h before a distinctly separate secondary flow-path. The overall volumetric efficiency of the clogged system was 71% and the hydrology was simulated using a dual-path, dead-zone storage model. It is concluded that uneven inlet distribution, continuous surface loading and high rhizosphere resistance is responsible for the clog formation observed in this system. The average inlet hydraulic conductivity was 2 m d^{-1}, suggesting that current European design guidelines, which predict that the system will reach an equilibrium hydraulic conductivity of 86 m d^{-1}, do not adequately describe the hydrology of mature systems.

1. Introduction

Treatment Wetlands (TWs) have become an established technology choice in the UK for the treatment of wastewaters in remote locations. Over 1200 systems have been installed over the last 20 years – predominantly horizontal, sub-surface flow (HSSF) systems used for the tertiary treatment (i.e. polishing) of wastewater (Cooper, 2007). Such HSSF TWs consist of a bed of porous gravel, in which the wastewater is subject to the correct conditions for final purification. However, the cleaning process results in the gradual clogging of the subsurface, and thus deterioration of hydraulic conductivity

* *Corresponding author*. Tel.: +44(0)121 204 3724.
E-mail address: knowlesp@aston.ac.uk (P.R. Knowles).
0043-1354
doi:10.1016/j.watres.2009.09.028

Table 1 – Hydraulic conductivity measurements and system details reported in previous studies of gravel bed HSSF TWs.

Reference	System name	Treatment type	Conductivity (inlet)[a] ($m\,d^{-1}$)	Conductivity (outlet)[a] ($m\,d^{-1}$)	Method
Fisher, 1990	Scripus	Secondary	1800	25000	Level survey
	Typha	Secondary	2500	25000	Level survey
	Control	Secondary	2500	25000	Level survey
Kadlec and Watson, 1993	Benton Cell 3	Secondary	2500	27500	Level survey
Sanford et al., 1995a	Bed 4	Landfill Leachate	4150	3370	Level survey
Drury and Mainzhausen, 2000	Cell 1	Acid drainage	6	3500	Level survey
	Cell 2	Acid drainage	6	3500	Level survey
Watson and Choate, 2001	Jones	Secondary	1000	5400	Level survey
	Gray	Secondary	10200	8100	Level survey
	Terrell	Secondary	4900	4700	Level survey
	Snelling	Secondary	85	325	Level survey
Caselles-Osorio et al., 2007 [a]	Verdu 1	Secondary	2	12	Falling head
	Verdu 2	Tertiary	25	61	Falling head
	Alfes	Secondary	7	2	Falling head
	Corbins	Primary	2	200	Falling head
	Almaret N	Secondary	1	87	Falling head
	Almaret S	Secondary	1	82	Falling head
Pedescoll et al., 2009	Verdu	Secondary	20	45	Falling head
	Corbins	Secondary	3	55	Falling head

a Values are width averaged.

over time (Wallace and Knight, 2006). The various symptoms that accompany clogging in HSSF TWs are widely documented and include surface sludge accumulations, overland flow, poor reed growth and weed infestation (Batchelor and Loots, 1997; Caselles-Osorio et al., 2007; Cooper et al., 2005; Fisher, 1990; Kadlec and Watson, 1993; Maloszewski et al., 2006; Rousseau et al., 2005; Watson et al., 1990). Indeed, such occurrences have been reported for many HSSF TWs in the UK, with Cooper et al. (2008) reporting that from a survey of 255 SSF TWs (82% of which were HSSF tertiary treatment systems) almost 30% exhibited surface flow over most of the bed, and over 50% displayed weed colonisation across at least one quarter of the bed surface. Additionally, it was not unusual to find surface sludge accumulations exceeding 150 mm at the inlet and 40 mm at the outlet. Rousseau et al. (2005) made similar observations in their survey of 12 UK

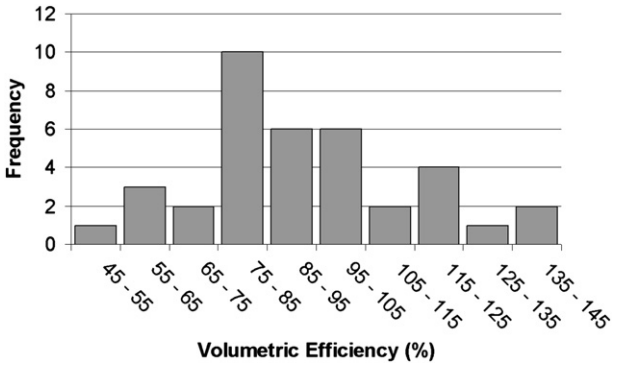

Fig. 1 – Frequency Distribution of the Volumetric Efficiency measured in 37 HSSF TWs, by comparison of observed and design Hydraulic Residence Times. Adapted from Kadlec and Wallace (2008).

based HSSF stormwater TWs, reporting that the vast majority of them had experienced sludge build-up over the entire surface of the bed. Despite vast anecdotal evidence the exact mechanisms of clogging are not wholly understood, Blazejewski and Murat-Blazejewska (1997) and Platzer and Mauch (1997) summarised the numerous physical design parameters and operational variables responsible. These include wastewater solids characteristics, subsurface media characteristics and choice of batch or continuous operating mode.

According to European Design Guidelines (Cooper, 1990), HSSF TWs which employ gravels with sizes of 3–12 mm will mature to reach an equilibrium hydraulic conductivity of about 86.4 $m\,d^{-1}$. However, the non-cohesive nature of gravel makes it difficult to remove representative samples from the field to test this hypothesis using a laboratory permeameter. Ranieri (2003) used an *in-situ* permeameter called the Guelph Permeameter (Reynolds and Elrick, 1986) to survey a gravel bed HSSF TW in Italy finding values ranged from 190 to 610 $m\,d^{-1}$, although these values are above the practical measurement range of the device (1–90 $m\,d^{-1}$). Though Langergraber et al.(2003) used the Guelph Permeameter to measure hydraulic conductivity within a Vertical Flow Subsurface Treatment Wetland, their system contained sand in addition to gravel resulting in a hydraulic conductivity low enough for measurement with this instrument. Indeed, most *in-situ* permeability tests are intended for cohesive, unsaturated geological material with hydraulic conductivities far below those usually measured in gravel beds (ASTM-D5126, 2004).

Consequently, the hydraulic conductivity profile of the wetland has usually been estimated from Darcy's Law, by measuring the corresponding water table height at different points in the bed. Conclusions generally agree that the inlet zone becomes more clogged than the remainder of the system

Table 2 – Details of the site used to trial the proposed combination of experimental methods.

Moreton Morrell	
Latitude./Longitude.	52.20/-1.55
Test Date	June 2008
Age at test (months)	177
Treatment Type	Tertiary municipal
Dimensions (m)	15 L × 15 W × 0.6D
Substrate	3–9 mm gravel
HLR ($m^3\ d^{-1}$)	175 $m^3\ d^{-1}$
Inlet Arrangement	4* Vertical risers
Effective gravel diameter d_{10} (mm)	2.6
Gravel median diameter d_{50} (mm)	5.2
Gravel uniformity coefficient	2.11
Particle size distribution gradation coefficient	1.48
Gravel clean hydraulic conductivity ($m\ d^{-1}$)	2100

due to the high degree of solids removal in this region (Table 1). However, this method may not accurately determine the extent of clogging, as Darcy's Law cannot take into account the varying thickness of the water table resulting from the groundwater energy balance and also requires that the flow field is saturated (Bear, 1979). For small hydraulic gradients, the accuracy with which the water table can be measured is limiting (Sanford et al., 1995a). Further, although this method may estimate the bulk resistance offered by the wetland media in the direction orthogonal to flow, it does not detect whether clogging varies vertically (Dittrich, 2006). Recently, methods to directly measure substrate permeability have been employed by Caselles-Osorio et al.(2007) and Pedescoll et al. (2009) on full-scale HSSF TWs in Spain, by utilising an *in-situ* falling head permeability test (NAVFAC, 1986). This method removes the uncertainty involved in estimating substrate conductivity from water-table surveys. Knowles and Davies (2009) have proposed a new method for the *in-situ* measurement of high conductivity materials, which recreates the constant head permeability test (BS-ISO-17313, 2004) *in-situ*. This allows both the magnitude and position of clogging within the subsurface to be determined.

The hydrodynamics that correspond to the developed clogging profile can be determined by tracer studies. Through this several authors have established that multiple preferential flow paths can exist through the wetland subsurface (Batchelor and Loots, 1997, Maloszewski et al., 2006). Regarding the UK condition, systems highly loaded with solids may develop separate overland and sub-surface flow fractions due to a high degree of surface clogging (Batchelor and Loots, 1997; Christian, 1990; Sanford et al., 1995b). Secondly, several authors have observed that sub-surface flow will often short-circuit across the bottom of the bed concluding that the greater resistance to flow offered by the rhizosphere is responsible for this (Breen and Chick, 1995; Fisher, 1990; Waters et al., 1993). This likelihood is supported by Tanner et al. (1998), who confirmed during a 5 year study of a dairy effluent HSSF TW that the clogging contribution from vegetation could be 1–2 times more significant than that from wastewater. Further studies of this system identified that the organic matter was highly refractory in nature and mainly accumulated in the top 100 mm of media (Nguyen, 2001), possibly explaining the 50% reduction in observed hydraulic retention time. Indeed, hydraulic inefficiency caused by clogging and short-circuiting is a common facet of TW performance. This is emphasised in Fig. 1 which shows that from a survey of tracer tests performed on 37 HSSF TWs, 29 underperformed with an average volumetric efficiency of 91% (Kadlec and Wallace, 2008).

The two tracer materials which have been used predominantly in previous wetland studies are bromide salts and Rhodamine Water Tracer, although each noted to have certain limitations (Flury and Wai, 2003). For example, Rhodamine dye is only said to behave conservatively if the TW is small, shallow (less than 0.6 m) and with a hydraulic residence time of less than one week (Lin et al., 2003). However, Rhodamine has obvious advantages over more conservative tracers, such as radioactive or biologically based alternatives, in that it has low eco-toxicity and will eventually photochemically destabilise, making it a good choice for ecological applications. Another advantage of Rhodamine is that it is easy to measure *in-situ* with relatively inexpensive equipment, making it the choice for this study and many previous TW hydraulics studies (Bhattarai and Griffin Jr, 1999; Holland et al., 2004; Shilton and Prasad, 1996; Simi and Mitchell, 1999).

This paper details complementary methods that have been developed to assess the impact of clogging at a mature HSSF TW located in Moreton Morrell, Warwickshire, UK, under the jurisdiction of Severn Trent Water plc. One method allows the

Fig. 2 – Photographs detailing the more prominent findings at the site, including a) Completely clogged inlet distributors, b) Surface sludge layers up to 200 mm thick at the inlet, c) two water levels at certain points in the system, representing disconnected overland and sub-surface flows.

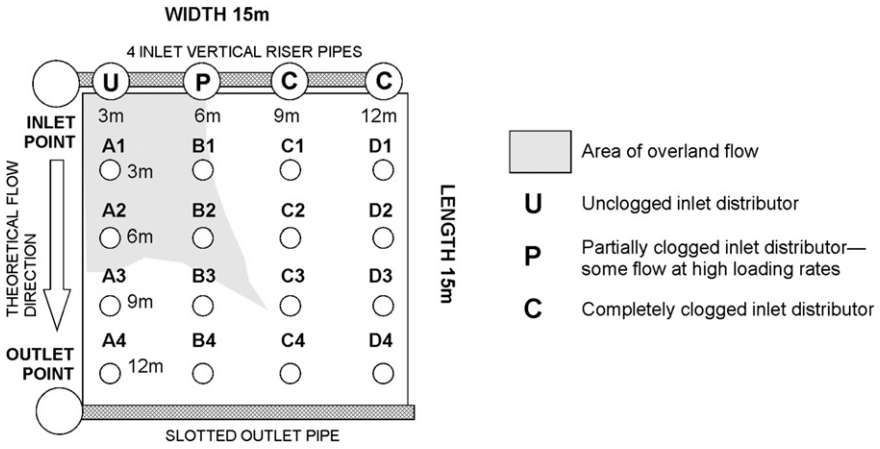

Fig. 3 – Plan view of Moreton Morrell tertiary treatment TW in Warwickshire (UK), showing the major design features, operational observations, and the locations of sampling points used during the experiments (drawing not to scale).

in-situ measurement of substrate hydraulic conductivity at different longitudinal, transverse and vertical locations within the bed, so that the exact position of clogging within the subsurface can be located. The second method is a multi-point tracer study to confirm that flow follows the path of least resistance. The Rhodamine break-through curve is also monitored at the outlet and levelling surveys are performed to explore the physical characteristics of the system. It is intended that the tests performed will elucidate the mature hydrology of this type of Treatment Wetland, and reveal details of the internal clogging mechanism.

2. Methods

2.1. Site description

Information regarding the site is given in Table 2. The site is almost 15 years old and as of June 2008 had a fully established macrophyte root network (*Phragmites australis*). Symptoms of hydraulic maturity were evident including inlet distributor pipes with variable degrees of clogging such that width distribution was uneven (Fig. 2a), and a thick surface sludge layer towards the inlet (Fig. 2b). It was assumed these factors were responsible for overland flow across a quarter of the bed surface (Cooper et al., 2008). As shown in Fig. 2c, the water table height was often below the level of any surface waters that were present at that point, suggesting a vertical head loss existed between the two water levels. Fig. 3 details the major design features of the site, and shows the location of the sampling points from which results were collected.

Using water levelling techniques a survey of the test site was performed, measuring the relative heights of the surface sludge layer, gravel surface, and water table surface, at each sampling point. Kadlec and Watson (1993) quote the accuracy of their standard water survey technique to ±10 mm. To try and improve the accuracy of the method for this study, the location of the water surface was established using a digital

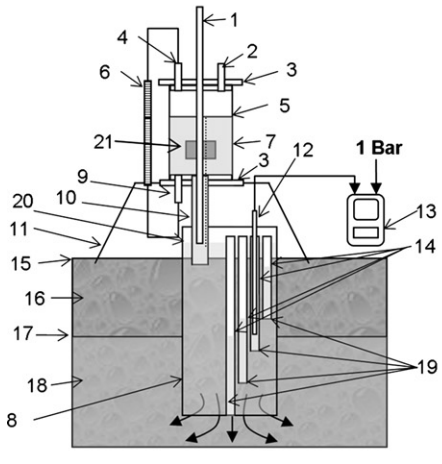

1. Air Inlet Pipe
2. Filling port
3. End cap
4. Air Port
5. Fluid Level in reservoir
6. Graduated measuring tube
7. Reservoir
8. 50cm long Permeameter Cell
9. Drain Port
10. Down pipe
11. Tripod
12. Graduated Depth Gauge
13. Digital Differential Manometer
14. Levels in manometer takeoff tubes
15. Gravel Surface
16. Unsaturated gravel
17. Free water surface
18. Saturated gravel
19. Manometer takeoff tubes
20. Mariotte Siphon Level
21. Stop cap

Fig. 4 – Experimental set-up (left) for in-situ determination of the hydraulic conductivity of highly porous media (not to scale) and the apparatus installed at a HSSF TW in the UK (right). Reservoir stands approx. 1 m off the ground. Reproduced from Knowles and Davies (2009).

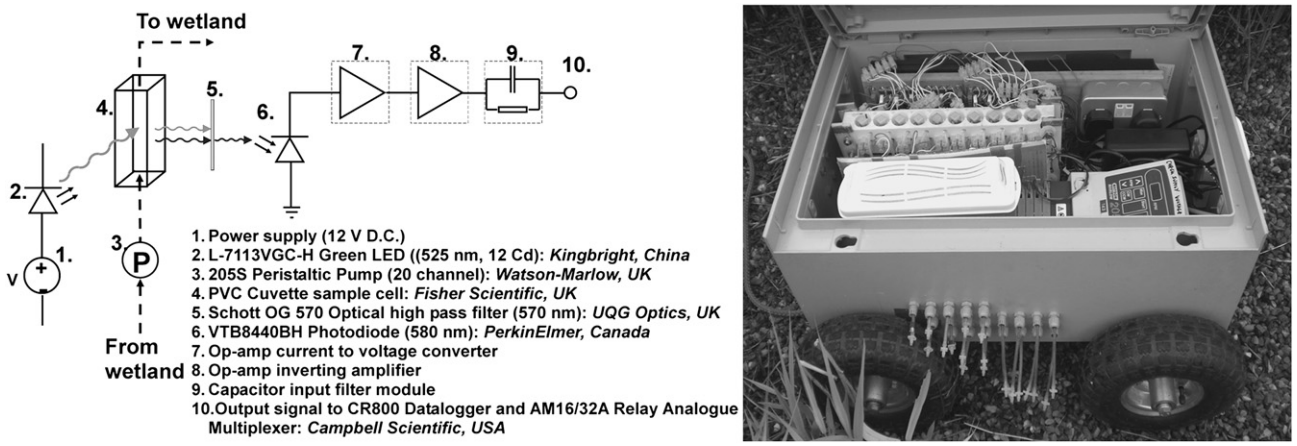

Fig. 5 – Schematic representation of one channel from the portable, multi-channel fluorimeter, showing the major opto-electronic and hydraulic modules involved in the design (left) and the multi-channel, in-situ fluorimeter installed at a HSSF TW in the UK (right).

manometer (Kane 3100-1, Kane International, Herts., UK). Through this, the associated error with each measurement is approximated as ±5 mm, mainly arising from human error in misreading graduated scales. All readings were made relative to an arbitrary datum which represents the bottom of the bed at the outlet. To set this it was assumed that the gravel depth was 0.6 m at the outlet and that the system was built with a bottom slope of 0.5%, following the European Design Guidelines being employed when it was constructed (Cooper, 1990).

2.2. *Hydraulic conductivity*

The test monitors the discharge of a constant head of water through a 400 mm (L_{CELL}) core of substrate, contained within the walls of a 160 mm diameter permeameter cell with cross-sectional area A_{CELL}. The level of water in the cell is kept constant by a Mariotte Siphon activated water reservoir, similar in principle to the Guelph Permeameter (Reynolds and Elrick, 1986) but enlarged to make it suitable for applications in higher conductivity media such as gravel (86.4 m d^{-1} to 86400 m d^{-1}). From this point on, all numbers in square brackets refer to those labels indicated on Fig. 4 (left), which illustrates the major components of the experiment. Four manometer take off tubes [19] (11.5 mm ID tubes ranging from 200 to 500 mm length in 100 mm increments), are inserted into the gravel core prior to the experiment commencing, to provide takeoff points at 100, 200, 300 and 400 mm depths into the gravel core. Using a digital differential manometer [13]

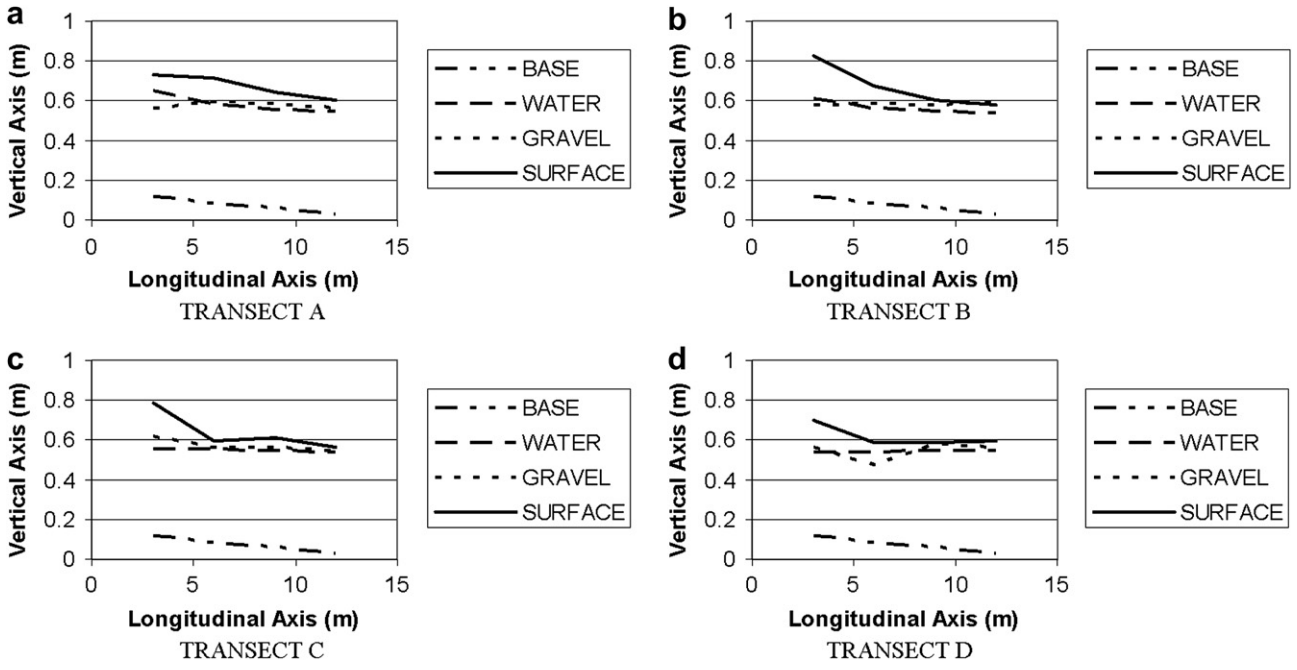

Fig. 6 – The longitudinally varying profile of the four transverse sampling transects A–D, detailing the relative height of the surface, water, gravel and base levels.

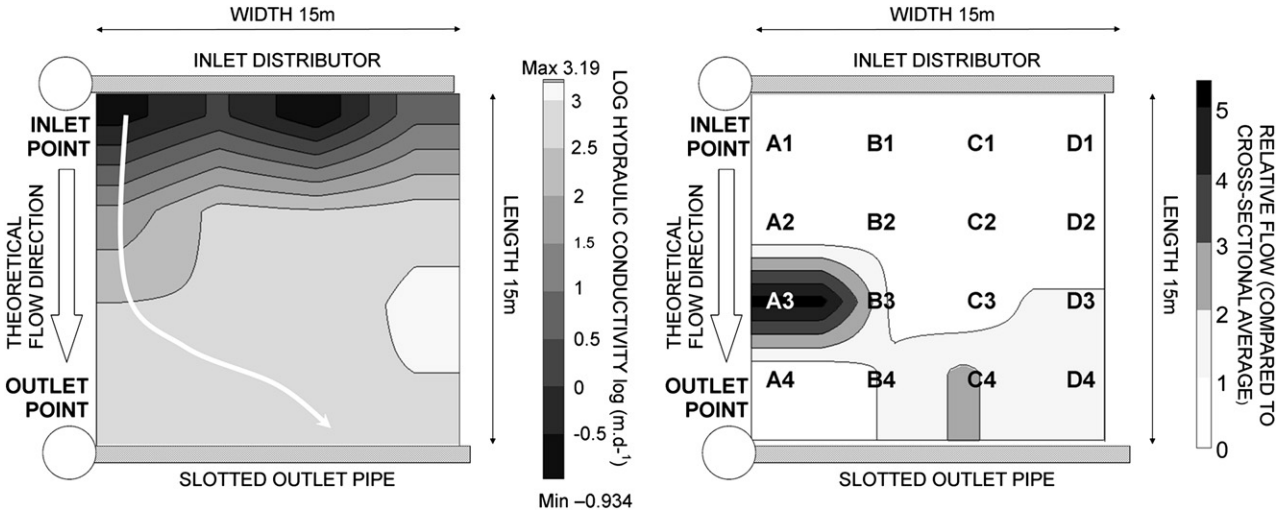

Fig. 7 – (Left) The variation in hydraulic conductivity over the surface of the TW surveyed at Moreton Morell. The darker regions represent those of lower hydraullo conductivity (greater clogging) and the lighter regions those of higher conductivities (lesser clogging). A possible primary preferential flow path is indicated with a white arrow , based on the equipotential lines across the permeability contours. (Right). The corresponding flow fraction measured at the 500 mm depth plane within the TW subsurface as a result of the clogging. The darker regions represent those that receive more flow (Figures produced using COMSOL Multiphysics 3.4-COMSOLAB).

with a 500 mm graduated depth gauge [12] in each take off tube, it is possible to determine the static [17] and dynamic [14] water levels, thus allowing the vertical head loss across each 100 mm section (h_n) to be measured. By monitoring the discharge of water ($\dot{q}$) from the reservoir [5,6], in keeping the permeameter head (h_T) constant, it is possible to calculate the permeability of the gravel core (k_T) using Darcy's Law Eq. (1).

$$k_T = \frac{\dot{q} \times L_{CELL}}{A_{CELL} \times h_T} \quad (1)$$

Subsequently the permeability of each 100 mm section (k_n) can be found Eq. (2).

$$k_n = \frac{h_T \times k_T}{4h_n} \quad (2)$$

The test provides vertical conductivity profiles, although by interpolating between sample points it would be possible to predict a horizontal conductivity profile. This is based on the assumption that flow would behave identically in all directions. Fig. 4 (right) gives a photo of the experimental setup at a TW in South Warwickshire. The apparatus cost just over £1000 (€1270) in 2008; approximately £100 (€130) to construct the Mariotte siphon reservoir and £900 (€1070) for the purchase of four digital manometers (Knowles and Davies, 2009). Experience has shown that obtaining one set of results can take between 20 min and one hour, depending on the degree of clogging. The test was performed at each sampling point indicated on Fig. 3.

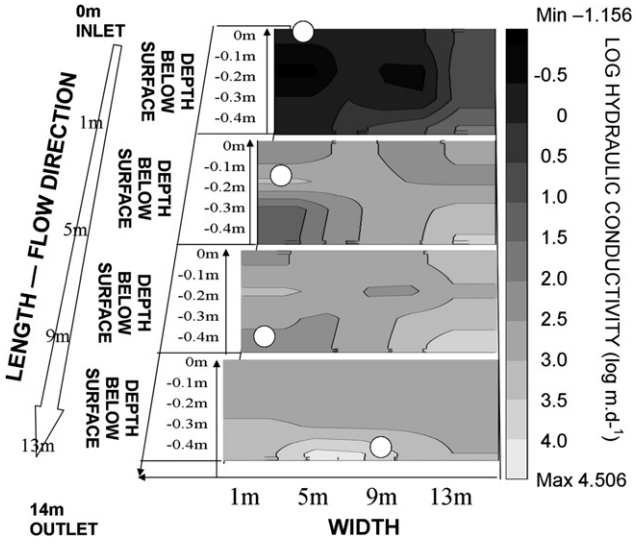

Fig. 8 – Linearly interpolated hydraulic conductivity values for five transverse cross sections at Moreton Morell TW. The darker regions represent those of lower hydraulic conductivity (greater clogging) and the lighter regions those of higher conductivities (lesser clogging). A possible primary preferential flow path, which snakes vertically and transversely, is indicated with a white circles, based on the equipotential lines across the permeability contours. (Figures produced using COMSOL Multiphysics 3.4-COMSOLAB).

2.3. *Tracer studies*

In response to there being no affordable proprietary fluorimeter for synchronous measurement from a matrix of sampling points, a novel multi-channel fluorimeter was created. The fluorimeter contains 20 separate opto-electronic modules, each based around a 570 nm high pass filter, photodiode with peak sensitivity at 580 nm, and an 18000 mCd LED with peak wavelength at 525 nm. These components correspond to the

Table 3 – Parameters derived from the breakthrough curves of each sampling point, studied using the multi-point fluorimeter. The hydraulic efficiency factor and short-circuiting factor are defined according to Persson et al.(1999) and Ta and Brignal (1998) respectively.

	A1	A2	A3	A4	B1	B2	B3	B4	C1	C2	C3	C4	D1	D2	D3	D4
Relative Flow Fraction	0.57	0.01	5.40	0.30	0.24	0.71	0.67	1.20	0.46	0.74	0.00	2.22	0.00	NR	1.23	1.25
Peak Time (d)	0.11	0.03	0.03	0.09	0.01	0.03	0.02	0.03	0.10	0.07	0.05	0.19	0.02	NR	0.33	0.13
Centroid Time (d)	0.08	0.17	0.17	0.13	0.14	0.16	0.05	0.19	0.09	0.16	0.09	0.17	0.04	NR	0.31	0.17
Theoretical Centroid Time (d)	0.07	0.14	0.22	0.29	0.07	0.14	0.22	0.29	0.07	0.14	0.22	0.29	0.07	NR	0.22	0.29
Volumetric Efficiency	1.06	1.17	0.76	0.45	1.92	1.14	0.24	0.64	1.22	1.11	0.41	0.57	0.61	NR	1.41	0.58
Hydraulic Efficiency Factor	1.45	0.16	0.21	0.72	0.08	0.17	0.33	0.15	1.18	0.41	0.51	1.18	0.47	NR	1.08	0.74
16% Breakthrough Curve (d)	0.03	0.04	0.07	0.08	0.02	0.06	0.01	0.09	0.06	0.07	0.04	0.09	0.02	NR	0.31	0.09
50% Breakthrough Curve (d)	0.07	0.16	0.16	0.11	0.13	0.16	0.03	0.18	0.09	0.15	0.10	0.16	0.03	NR	0.33	0.16
84% Breakthrough Curve (d)	0.10	0.29	0.25	0.19	0.25	0.25	0.09	0.27	0.10	0.24	0.13	0.22	0.07	NR	0.35	0.24
Short-Circuiting Factor	0.45	0.23	0.44	0.71	0.13	0.38	0.40	0.47	0.64	0.43	0.43	0.57	0.50	NR	0.94	0.57

fluorescing properties of the Rhodamine WT used in the experiments (Tolbest, UK), which has excitation and emission wavelengths at 556 nm and 580 nm respectively. Each module produces a voltage proportional to the concentration of Rhodamine passing through a flow-through PVC cuvette. The sensitivity of each channel is adjustable, and the practical resolution, as imposed by the signal to noise ratio, would allow a useful detection range of about 10 parts per billion (ppb) of Rhodamine in water. The sample fluid is drawn from different points within the TW aquatic environment using a 20 channel peristaltic pump; each channel connected to a different opto-electronic module. Along with data logging equipment, all of these components are mounted in a modified IP66 rated, weatherproof enclosure (Sarel, Italy) which can be wheeled onto the monitoring site of interest. More information regarding these components is included in Fig. 5 (left), which gives a schematic representation of one channel. Fig. 5 (right) is a photograph of the interior of the multi-channel fluorimeter at a TW in South Warwickshire.

A 5 ml single-shot impulse of concentrated Rhodamine WT solution was added to the inlet manifold, upstream of the wetland cell. Lengths of 20 m silicon tubing with an ID of 3 mm (Fisher Scientific, UK) were attached to 16 of the fluorimeter channels, with one tube originating from each sampling point. The tube openings were submersed to 0.5 m below the gravel surface to investigate the nature of the flow field at this height. Each peristaltic pump channel was set to deliver 0.2 ml s^{-1} through the fluorimeter. The machine discharged the analysed water directly onto the centre of the bed surface as it was considered the total discharge (0.003 l s^{-1}) was significantly small compared with the flow though the wetland (2 l s^{-1}) to have negligible impact on downstream fluorescence measurements. The Rhodamine breakthrough curve was measured at the outlet using a Cyclops 7 submersible fluorimeter (Turner Designs, USA).

3. Results

3.1. Site survey

Fig. 6 shows the longitudinally varying profile of the four transverse sampling transects A–D. Variations in hydraulic gradient across the four transects were between 109 mm (transect A) and 7 mm (and transect D) relating to the uneven flow distribution through the inlet risers. The equilibrium saturated water table height of the system is consistently below the bed surface, despite the appearance of overland flow. The water table is located below the gravel surface at all points apart from in the first 5 m of transects A and B, where it is located within the sludge layer. It can be seen from Fig. 6b that towards the inlet of transect B, the depth of sludge that has accumulated on the surface of the gravel exceeds 200 mm. The depth of surface sludge is generally greatest at the inlet and becomes progressively shallower towards the outlet.

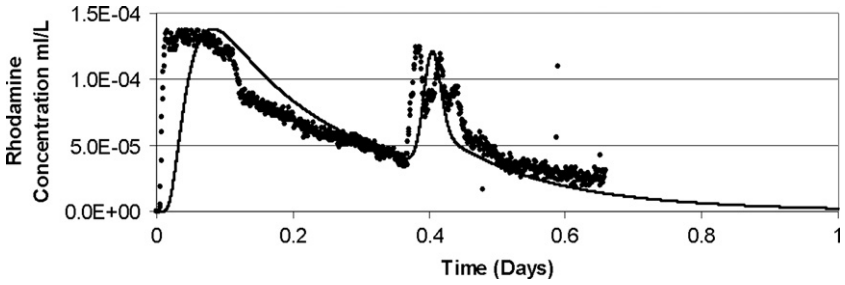

Fig. 9 – The obtained Rhodamine WT Residence Time Distribution Curve (dotted line) and the fitted Aggregated Dead-Zone Model (solid line).

Table 4 – Hydraulic parameters for the various flow paths derived from the outlet residence time distribution, and parameters used to fit the dead-zone storage model. The hydraulic efficiency factor and short-circuiting factor are defined according to Persson et al. (1999) and Ta and Brignal (1998) respectively.

Hydraulic loading rate	$m^3\,d^{-1}$	175			
Theoretical residence time	*d*	0.36			
Total tracer injected	*ml*	5			
			Single path	Overland path	Subsurface path
Mean Residence Time	*d*		0.26	0.21	0.46
Peak Time	*d*		0.04	0.04	0.59
16% Tracer Recovery Time	*d*		0.06	0.05	0.39
84% Tracer Recovery Time	*d*		0.45	0.40	0.55
Total Tracer Recovered	*ml*		3.83	3.15	0.68
Flow-Split			1	0.82	0.18
Volumetric Efficiency			0.71	0.59	1.27
Number of CSTRs (N)			1.20	1.20	−0.85
Hydraulic Efficiency (λ)			0.17	0.21	1.29
ShortCircuiting (S)			0.27	0.31	0.90
ADZ Model parameters, *Estimated from method of moments					
*Dispersion	$m^2\,s^{-1}$			4.E-03	8.E-05
*Velocity	$m\,s^{-1}$			8.E-04	4.E-04
*Effective area				0.69	0.10
Storage transfer coefficient	*s*			40000	30000

3.2. Hydraulic conductivity

Fig. 7 (left) shows how the hydraulic conductivity through each 0.4 m long gravel core varies across the bed surface (note the shading bar is a logarithmic scale). The darker regions represent those of lower hydraulic conductivity (greater clogging) and the lighter regions those of higher conductivities (lesser clogging). The minimum value of 0.1 m d^{-1} was measured at inlet point C1 and the maximum of 1550 m d^{-1} measured at outlet point D3. Width average conductivities for the four transects orthogonal to flow were 2, 343, 650 and 800 m d^{-1}, from inlet to outlet respectively. The order of magnitude of the inlet values are in good agreement (Table 1) with other studies that have directly measured substrate conductivity (Caselles-Osorio et al., 2007; Pedescoll et al., 2009). According to the contours on Fig. 7 (left), the overland flow in the system seems to correspond to wherever the hydraulic conductivity is less than 100 m d^{-1}.

Fig. 8 demonstrates four transverse slices through the TW, developed from the 3D permeability results, which elucidates the locality of clogging. Values at the surface of the inlet zone across transects A–C were below 0.5 m d^{-1}. This explains the poor percolation of the influent waters at the inlet region and the resulting overland flow. Beyond the inlet the effect of the rhizosphere is to keep the conductivity between 100 and 1000 m d^{-1}, whilst below the rhizosphere (especially towards the outlet), values are generally greater than 1000 m d^{-1}. Overall, values varied by 6 orders of magnitude, from a minimum of 0.04 m d^{-1} at a 200 mm depth below point B1, to a maximum of 40,000 m d^{-1} at a 400 mm depth below point C4. The effect of poor inlet distribution is also evident in Fig. 8. Values along transect D are at least twice as high as values measured elsewhere, corresponding to the negligible influent distribution along this transect.

3.3. Flow pattern visualisation

Fig. 7 (right) compares the total dye detected at each point with the average detected over the 500 mm vertical plane. This indicates the relative location of preferential flow-paths and dead-zones as values greater and less than one respectively. An instrument error meant no information was collected for point D2. The biggest preferential flow-path is detected at point A3 (5.4 times the average flow) which roughly coincides with the area where overland flow ceases. In contrast, upstream points A1 and A2 have very little involvement in the flow field, confirming observations that the majority of the flow short-circuits over the surface sludge until it can infiltrate into the subsurface and follow the path of least resistance below the rhizosphere. In accordance with the hydraulic conductivity results, flow follows the path of least resistance downstream from point A3, by steering towards points B3, B4, C4 and D4; perhaps avoiding a clogged outlet collector at point A4 (Cooper et al., 2008). Calculation of the volumetric efficiency emphasises the inefficiency created by this flow regime. Downstream points 3 and 4 at transects A B and C have values between 24% and 76% efficiency (Table 3) reflecting the premature passage of the RTD centroid where the overland flow secedes. Upstream points 1 and 2 at these transects consistently have volumetric efficiencies greater than 100% which is attributable to the low infiltration rates through the sludge layer at the inlet.

The outlet RTD very clearly indicates the existence of two major flow-paths through the HSSF TW (Fig. 9) which have been partitioned according to the parameters reported in Table 4. The first path to arrive at the outlet corresponds to the overland flow that short-circuits to point A3, carrying 82% of the flow and arriving after only 1 h. The second represents the highly retarded flow-path from upstream percolations into

Table 5 – Suggested design guidelines applicable to the gravel media considered in this study, for equilibrium hydraulic conductivity at the inlet zone.

Source	Range of applicable media (mm)	Predicted hydraulic conductivity ($m\,d^{-1}$)
EC/EWPCA (1990)	5–10	86
TVA (1993)	3–6	2600
ÖNORM B l2505(1997)	4–8	518
IWA (2000)	3–16	1000

the subsurface which arrives almost 8 h later than the overland flow path. The mean residence times of these two paths were 0.21 and 0.46 days respectively, giving an overall volumetric efficiency of 71% when compared with the nominal residence time of 0.36 days. Tracer recovery was 77% with the loss mainly attributed to adsorption.

4. Discussion

According to the water-table survey, a flow-rate of $2\,l\,s^{-1}$ through the wetland produced a hydraulic gradient of 0.9%. If calculated using Darcy's Law, this would correspond to a hydraulic conductivity of $140\,m\,d^{-1}$. Despite the clogging evident from overland flow, this would suggest that system conductivity is still greater than the equilibrium guideline of $86.4\,m\,d^{-1}$ which was employed when it was designed (EC/EWPCA, 1990). However, this figure represents the overall hydrology of the system and does not describe the six orders of magnitude variation in substrate hydraulic conductivity and corresponding short-circuiting that was measured between the inlet and outlet. Table 5 indicates that the guideline value used is the most conservative available when compared to equivalent guidelines published in various manuals and regulatory documents from around the world. This calls into question the current basis for the hydraulic design of HSSF TWs in the UK.

A dual-path, dead-zone storage model was used to describe the shape of the outlet RTD. Multiple flow-path models

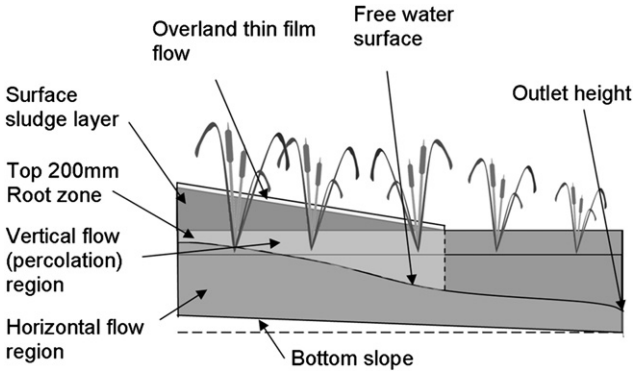

Fig. 10 – Representation of the hydrological regime prevalent in UK, HSSF TWs for the tertiary treatment of municipal wastewater. Diagram depicts a transverse cross-section and is not to scale.

(Chazarenc et al., 2003; Maloszewski et al., 2006; Wang and Jawitz, 2006) and dead-zone storage models (Martinez and Wise, 2003; Wang and Jawitz, 2006; Werner and Kadlec, 2000) have been used previously to describe the multiple peaks and weighted significance of the tail observed in HSSF TW breakthrough curves (Kadlec and Wallace, 2008). However, there is no knowledge of them being combined to describe flow through these systems. This was achieved using the MS Excel based HUSKY 1 code as formulated by Hellweger (2005), and the modelling parameters indicated in Table 4. Three of the model parameters were estimated by analysing the RTDs using the method of moments, leaving only the storage transfer coefficient to be optimised. The successfully fit transfer coefficients are similar to values used by Wang and Jawitz (2006) of 40000 s. The model is thought to adequately describe the obtained breakthrough curve (Fig. 9), despite the slight misiming of the 1st peak.

Fig. 10 describes the hydrological regime within a mature HSSF TW with surface loading, based on the observations made during the study. Major features include a low permeability surface sludge layer which is deepest at the inlet due to preferential solids accumulation in this region, a low permeability region in the top 200–300 mm of media associated with the bulk of the rhizosphere, separate equilibrium water levels in the system related to overland flow across a vertical percolation region and the water table resulting from horizontal flow respectively, and finally a non-linearly varying water table surface. Inlet clogging to the point where surface flow ensues may be unavoidable given the current design configuration of UK systems. The main factor responsible for the way that clogging has developed at Moreton Morrell is poor inlet distribution causing preferential sludge and detritus accumulation and overland flow down one side of the bed. Systems built in the UK since Moreton Morrell have incorporated improved inlet distributors (Griffin et al., 2008), such as troughs with numerous v-notch weirs, to try and reduce the problems associated with riser pipes (Cooper et al., 2008) However, poor inlet distribution is not the only condition responsible for clogging and ponding of water on the surface of the bed. Tertiary systems in the UK have a higher areal hydraulic loading rate than secondary systems and the municipal wastewater that they receive is a combination of domestic and urban diffuse sources. During wet weather events the larger flows can overwhelm upstream processes causing washout of biological flocs and accumulated solids. These factors mean UK tertiary systems often receive a higher solids load than their secondary counterparts elsewhere in the world. Loading solids onto the bed surface increases the likelihood that the surface will seal; especially when the rhizosphere develops and reduces the pore diameter available for particle infiltration. American HSSF TW systems, such as those reported by Wallace and Knight (2006), utilise submersed inlet distributors which load the influent wastewater over the entire cross-sectional area orthogonal to flow, reducing the tendency of the surface to seal near the inlet. The continuous application of secondary wastewater will also promote surface clogging. In French Vertical Flow systems, primary wastewater is intermittently dosed onto the bed surface, giving opportunity for the surface sludge layer to dry out. This prevents terminal

ponding despite the comparatively high solids loading in French systems (Chazarenc and Merlin, 2005).

5. Conclusions

Complementary *in-situ* hydraulic conductivity and Rhodamine dye tracing experiments have been successfully employed to model the hydraulic conditions in a clogged, gravel bed, tertiary wastewater treatment wetland. The *in-situ* constant head permeameter method revealed that the hydraulic conductivity at the inlet was of the order of 1 m d^{-1}, compared to 2–3 orders of magnitude greater elsewhere. The ability to measure vertical variations in subsurface hydraulic conductivity established that the greatest resistance corresponded to the surface sludge and rhizosphere regions. The multi-point dye tracing technique confirmed that sub-surface flow vertically short-circuits below the rhizosphere following the path of least resistance. Almost 36% of the total flow detected at a 500 mm depth occurred at one point which roughly coincided with where overland flow terminated. The outlet RTD confirmed that two distinctly separate flow paths exist through the system: a primary overland path which constituted almost 80% of the flow field, and a secondary subsurface path that was heavily retarded in comparison to the overflow path. The nature of the clogging resulted in tracer detection at the outlet within one hour, and an overall system volumetric efficiency of 71%. A dual-path, dead-zone storage model was used to adequately describe the observed flow dynamics.

It can be concluded that observations of overland flow across one quarter of the bed are attributable to poor surface infiltration rates at the inlet and uneven influent distribution across the width. The hydraulic conductivity of the system generally decreases from inlet to outlet and from surface to base. Even the most conservative design guidelines overestimated the hydraulic conductivity of the fouled inlet media by a factor of 40. If, however, design guidelines were based on a hydraulic conductivity of 1 m d^{-1}, as measured here, this would result in impractically large wetland areas. Instead, it is recommend to design beds with large width to length ratios, such that the influent is distributed over a wider area, thus delaying terminal clogging. Subsequent work will compare a large cross-section of operational wetlands with a variety of ages, operating conditions and design characteristics that may help explain the clogging mechanism and allow guidelines to be stipulated which help maximise the longevity of these systems. A predictive finite element model will also be developed which will allow the correlation between the permeability and dye tracing results to be analysed in more detail.

Acknowledgements

This work was made possible thanks to joint funding from Severn Trent Water Plc. (UK) and a CASE studentship granted by the ESPRC UK (ref. CASE/CNA/06/28). The first author gratefully acknowledges Anna Pedescoll from the Technical University of Catalonia, Spain for her indispensable assistance whilst performing the site survey.

REFERENCES

ASTM-D5126, 2004. Standard Guide for Comparison of Field Methods for Determining Hydraulic Conductivity in the Vadose Zone. American Society for the Testing of Materials, West Conshohocken, PA, USA.

Batchelor, A., Loots, P., 1997. A critical evaluation of a pilot scale subsurface flow wetland: 10 years after commissioning. Water Science and Technology 35 (5), 337–343.

Bear, J., 1979. Hydraulics of Groundwater. McGraw-Hill, New York; London.

Bhattarai, R.R., Griffin Jr., D.M., 1999. Results of tracer tests in rock-plant filters. Journal of Environmental Engineering 125 (2), 117–125.

Blazejewski, R., Murat-Blazejewska, S., 1997. Soil clogging phenomena in constructed wetlands with subsurface flow. Water Science and Technology 35 (5), 183–188.

Breen, P.F., Chick, A.J., 1995. Rootzone dynamics in constructed wetlands receiving wastewater: a comparison of vertical and horizontal flow systems. Water Science and Technology 32 (3), 281–290.

BS-ISO-17313, 2004. Soil Quality. Determination of Hydraulic Conductivity of Saturated Porous Materials Using a Flexible Wall Permeameter. British Standards Institute.

Caselles-Osorio, A., Puigagut, J., Segu, E., Vaello, N., Granés, F., García, D., García, J., 2007. Solids accumulation in six full-scale subsurface flow constructed wetlands. Water Research 41 (6), 1388–1398.

Chazarenc, F., Merlin, G., 2005. Influence of surface layer on hydrology and biology of gravel bed vertical flow constructed wetlands. Water Science and Technology 51 (9), 91–97.

Chazarenc, F., Merlin, G., Gonthier, Y., 2003. Hydrodynamics of horizontal subsurface flow constructed wetlands. Ecological Engineering 21 (2–3), 165–173.

Christian, J.N.W., 1990. Reed bed treatment systems: experimental gravel beds at Gravesend – the southern water experience. In: Cooper, P.F., Findlater, B.C. (Eds.), Constructed Wetlands in Water Pollution Control. Cambridge, UK: Pergamon Press, Oxford, UK, pp. 309–319.

Cooper, P.F. (Ed.), 1990. European Design and Operations Guidelines for Reed Bed Treatment Systems. WRc, Swindon, UK.

Cooper, P., 2007. The Constructed Wetland Association UK database of constructed wetland systems. Water Science and Technology 56 (3), 1–6.

Cooper, D., Griffin, P., Cooper, P., 2005. Factors affecting the longevity of sub-surface horizontal flow systems operating as tertiary treatment for sewage effluent. Water Science and Technology 51 (9), 127–135.

Cooper, D., Griffin, P., Cooper, P.F., 2008. Factors affecting the longevity of sub-surface horizontal flow systems operating as tertiary treatment for sewage effluent. In: Vymazal, J. (Ed.), Wastewater Treatment, Plant Dynamics and Management in Constructed and Natural Wetlands. Springer, Dordrecht, The Netherlands, pp. 191–198.

Dittrich, E., 2006. Experiences on hydraulic performance of subsurface flow constructed wetlands. Pollack Periodica 1 (1), 53–66.

Drury, W.J., Mainzhausen, K., 2000. Hydraulic characteristics of subsurface flow wetlands, 2000 Billings Land Reclamation Symposium, Billings, MT, USA

EC/EWPCA, 1990. European Design and Operations Guidelines for Reed Bed Treatment Systems. WRc, Swindon, UK.

Fisher, P.J., 1990. Hydraulic Characteristics of Constructed Wetlands at Richmond, NSW, Australia. In: Cooper, P.F., Findlater, B.C. (Eds.), Constructed Wetlands in Water Pollution Control. Cambridge, UK: Pergamon Press, Oxford, UK, pp. 21–31.

Flury, M., Wai, N.N., 2003. Dyes as tracers for vadose zone hydrology. Reviews of Geophysics 41 (1), 1–2.

Griffin, P., Wilson, L., Cooper, D., 2008. Changes in the use, operation and design of sub-surface flow constructed wetlands in a major UK water utility. 11th International Conference on Wetland Systems for Water Pollution Control, Indore, India, 419–426.

Hellweger, F.L., 2005. Measuring and modeling large-scale pollutant dispersion in surface waters. Collection Systems Alexandria, Virginia, 812–835.

Holland, J.F., Martin, J.F., Granata, T., Bouchard, V., Quigley, M., Brown, L., 2004. Effects of wetland depth and flow rate on residence time distribution characteristics. Ecological Engineering 23 (3), 189–203.

Kadlec, R.H., Wallace, S., 2008. Treatment wetlands. In: Boca Raton, Fla.: CRC, second ed. Taylor & Francis, London [distributor].

Kadlec, R.H., Watson, J.T., 1993. Hydraulics and solids accumulation in a gravel bed treatment wetland. In: Moshiri, G.A.E. (Ed.), Constructed Wetlands for Water Quality Improvement: Conference: Selected Papers. Boca Raton: Lewis Pub, pp. 227–235.

Knowles, P.R., Davies, P.A. (2009) A method for the in-situ determination of the hydraulic conductivity of gravels as used in constructed wetlands for wastewater treatment. Desalination and water treatment, 1 (5), 257–266.

Langergraber, G., Haberl, R., Laber, J., Pressl, A., 2003. Evaluation of substrate clogging processes in vertical flow constructed wetlands. Water Science and Technology 48 (5), 25–34.

Lin, A.Y.C., Debroux, J.F., Cunningham, J.A., Reinhard, M., 2003. Comparison of rhodamine WT and bromide in the determination of hydraulic characteristics of constructed wetlands. Ecological Engineering 20 (1), 75–88.

Maloszewski, P., Wachniew, P., Czuprynski, P., 2006. Study of hydraulic parameters in heterogeneous gravel beds: constructed wetland in Nowa Słupia (Poland). Journal of Hydrology 331 (3–4), 630–642.

Martinez, C.J., Wise, W.R., 2003. Analysis of constructed treatment wetland hydraulics with the transient storage model OTIS. Ecological Engineering 20 (3), 211–222.

NAVFAC, 1986. Soil Mechanics. Design Manual 7.01. Naval Facilities Engineering Command, Alexandria, Virginia, USA.

Nguyen, L., 2001. Accumulation of organic matter fractions in a gravel-bed constructed wetland. Water Science and Technology 44 (11–12), 281–287.

Pedescoll, A., Uggetti, E., Llorens, E., Granés, F., García, D., García, J. (2009) Practical method based on saturated hydraulic conductivity used to assess clogging in subsurface flow constructed wetlands. Ecological Engineering, 35 (8), 1216–1224.

Platzer, C., Mauch, K., 1997. Soil clogging in vertical flow reed beds – mechanisms, parameters, consequences and solutions? Water Science and Technology 35 (5), 175–181.

Ranieri, E., 2003. Hydraulics of sub-superficial flow constructed wetlands in semi arid climate conditions. Water Science and Technology 47 (7–8), 49–55.

Reynolds, W.D., Elrick, D.E., 1986. A method for simultaneous in situ measurement in the vadose zone of field-saturated hydraulic conductivity, sorptivity and the conductivity-pressure head relationship. Ground Water Monitoring Review 6 (1), 84–95.

Rousseau, D.P.L., Horton, D., Griffin, P., Vanrolleghem, P.A., De Pauw, N., 2005. Impact of operational maintenance on the asset life of storm reed beds. Water Science and Technology 51 (9), 243–250.

Sanford, W.E., Steenhuis, T.S., Parlange, J.Y., Surface, J.M., Peverly, J.H., 1995a. Hydraulic conductivity of gravel and sand as substrates in rock-reed filters. Ecological Engineering 4 (4), 321–326.

Sanford, W.E., Steenhuis, T.S., Surface, J.M., Peverly, J.H., 1995b. Flow characteristics of rock-reed filters for treatment of landfill leachate. Ecological Engineering 5 (1), 37–50.

Shilton, A.N., Prasad, J.N., 1996. Tracer studies of a gravel bed wetland. Water Science and Technology 34 (4), 421–425.

Simi, A.L., Mitchell, C.A., 1999. Design and hydraulic performance of a constructed wetland treating oil refinery wastewater. Water Science and Technology 40 (3), 301–307.

Tanner, C.C., Sukias, J.P.S., Upsdell, M.P., 1998. Organic matter accumulation during maturation of gravel-bed constructed wetlands treating farm dairy wastewaters. Water Research 32 (10), 3046–3054.

Wallace, S.D., Knight, R.L., 2006. Small-Scale Constructed Wetland Treatment Systems: Feasibility, Design Criteria and O & M Requirements. Water Environment Research Foundation (WERF), Virginia, Alexandria.

Wang, H., Jawitz, J.W., 2006. Hydraulic analysis of cell-network treatment wetlands. Journal of Hydrology 330 (3–4), 721–734.

Waters, M.T., Pilgrim, D.H., Schulz, T.J., Pilgrim, I.D., 1993. Variability of hydraulic response of constructed wetlands. Proceedings – National Conference on Hydraulic Engineering, 406–411.

Watson, J.T., Choate, K.D., 2001. Hydraulic conductivity of onsite constructed wetlands. In: On-Site Wastewater Treatment, Proceedings of the Ninth National Symposium on Individual and Small Community Sewage Systems. Michigan, St. Joseph, pp. 631–648.

Watson, J.T., Choate, K.D., Steiner, G.R., 1990. Performance of constructed wetland treatment systems at Benton, Hardin and Pembroke, Kentucky, during the early vegetation establishment. In: Cooper, P.F., Findlater, B.C. (Eds.), Constructed Wetlands in Water Pollution Control. Cambridge, UK: Pergamon Press, Oxford, UK, pp. 171–182.

Werner, T.M., Kadlec, R.H., 2000. Wetland residence time distribution modeling. Ecological Engineering 15 (1–2), 77–90.